REPORT DOCUMENTATION PAGE

Form Approved
OMB No. 0704-01-0188

PLEASE DO NOT RETURN YOUR FORM TO THE ABOVE ADDRESS.

1. REPORT DATE *(DD-MM-YYYY)*	2. REPORT TYPE	3. DATES COVERED *(From - To)*
2003	Journal Article	

4. TITLE AND SUBTITLE

Multiecho processing by an echolocating dolphin

5a. CONTRACT NUMBER

5b. GRANT NUMBER

5c. PROGRAM ELEMENT NUMBER

6. AUTHORS

Richard A. Altes[1]
Lois A. Dankiewicz[2]
Patrick W. Moore[3]
David A. Helweg[4]

5d. PROJECT NUMBER

5e. TASK NUMBER

5f. WORK UNIT NUMBER

7. PERFORMING ORGANIZATION NAME(S) AND ADDRESS(ES)

[1]Chirp Corp.
8248 Sugarman Dr.
La Jolla, CA 92037

[2]SAIC
3990 Old Town Ave.
Ste. 208A
San Diego, CA 92110

[3]SSC San Diego
53560 Hull St.
San Diego, CA
92152-5001

[4]Pacific Island Ecosystems
Research Center
3190 Maile Wy, Rm. 408
Honolulu, HI 96822

8. PERFORMING ORGANIZATION REPORT NUMBER

9. SPONSORING/MONITORING AGENCY NAME(S) AND ADDRESS(ES)

10. SPONSOR/MONITOR'S ACRONYM(S)

11. SPONSOR/MONITOR'S REPORT NUMBER(S)

12. DISTRIBUTION/AVAILABILITY STATEMENT

Approved for public release; distribution is unlimited.

13. SUPPLEMENTARY NOTES

14. ABSTRACT

Bottlenose dolphins (*Tursiops truncatus*) use short, wideband pulses for echolocation. Individual waveforms have high-range resolution capability but are relatively insensitive to range rate. Signal-to-noise ratio (SNR) is not greatly improved by pulse compression because each waveform has small time–bandwidth product. The dolphin, however, often uses many pulses to interrogate a target, and could use multipulse processing to combine the resulting echoes. Multipulse processing could mitigate the small SNR improvement from pulse compression, and could greatly improve range-rate estimation, moving target indication, range tracking, and acoustic imaging. All these hypothetical capabilities depend upon the animal's ability to combine multiple echoes for detection and/or estimation. An experiment to test multiecho processing in a dolphin measured detection of a stationary target when the number N of available target echoes was increased, using synthetic echoes. The SNR required for detection decreased as the number of available echoes increased, as expected for multiecho processing. A receiver that sums binary-quantized data samples from multiple echoes closely models the N dependence of the SNR required by the dolphin. Such a receiver has distribution-tolerant (nonparametric) properties that make it robust in environments with nonstationary and/or non-Gaussian noise, such as the pulses created by snapping shrimp.

Published in *Journal of Acoustical Society of America*, Vol. 114, No, 2, August 2003.

15. SUBJECT TERMS

Echolocation
Signal-to-noise ratio (SNR)
Tursiops truncatus

16. SECURITY CLASSIFICATION OF:			17. LIMITATION OF ABSTRACT	18. NUMBER OF PAGES	19a. NAME OF RESPONSIBLE PERSON
a. REPORT	b. ABSTRACT	c. THIS PAGE			Patrick Moore, Code 2351
U	U	U	UU	12	19B. TELEPHONE NUMBER *(Include area code)* (619) 553-0888

Multiecho processing by an echolocating dolphin

Richard A. Altes[a)]
Chirp Corporation, 8248 Sugarman Drive, La Jolla, California 92037

Lois A. Dankiewicz
Science Applications International Corporation, 3990 Old Town Avenue, Suite 208A, San Diego, California 92110

Patrick W. Moore
SSC San Diego, Code 23502, 53560 Hull Street, San Diego, California 92152

David A. Helweg
Pacific Island Ecosystems Research Center, 3190 Maile Way, Room 408, Honolulu, Hawaii 96822

(Received 29 April 2002; revised 18 April 2003; accepted 12 May 2003)

Bottlenose dolphins (*Tursiops truncatus*) use short, wideband pulses for echolocation. Individual waveforms have high-range resolution capability but are relatively insensitive to range rate. Signal-to-noise ratio (SNR) is not greatly improved by pulse compression because each waveform has small time–bandwidth product. The dolphin, however, often uses many pulses to interrogate a target, and could use multipulse processing to combine the resulting echoes. Multipulse processing could mitigate the small SNR improvement from pulse compression, and could greatly improve range-rate estimation, moving target indication, range tracking, and acoustic imaging. All these hypothetical capabilities depend upon the animal's ability to combine multiple echoes for detection and/or estimation. An experiment to test multiecho processing in a dolphin measured detection of a stationary target when the number N of available target echoes was increased, using synthetic echoes. The SNR required for detection decreased as the number of available echoes increased, as expected for multiecho processing. A receiver that sums binary-quantized data samples from multiple echoes closely models the N dependence of the SNR required by the dolphin. Such a receiver has distribution-tolerant (nonparametric) properties that make it robust in environments with nonstationary and/or non-Gaussian noise, such as the pulses created by snapping shrimp. © *2003 Acoustical Society of America.* [DOI: 10.1121/1.1590969]

PACS numbers: 43.80.Lb, 43.66.Gf [WA]

I. INTRODUCTION

Active echolocation allows bottlenose dolphins (*Tursiops truncatus*) to investigate their surroundings using hearing (see Au, 1993 for review). Multiple broadband, short-duration acoustic "clicks" are emitted by the dolphin. Interaction of the emitted signals with an object causes echoes to return to the animal. Echo characteristics are influenced by the location, orientation, and physical attributes of the object. By listening to these returning echoes, dolphins are able to locate and identify elements in their environment that might be difficult to detect visually.

Because an echo is potentially generated for every click that impinges on an object, the amount of information available to the dolphin increases as more click–echo pairs are produced. Much research has focused on the information contained in the click–echo pair and how it is used by the dolphin (Au, 1993; Au *et al.*, 1988; Busnel and Fish, 1980; Helweg *et al.*, 1996; Nachtigall and Moore, 1988; Thomas and Kastelein, 1990). The manner in which multiple echoes clarify or add information, and how the dolphin utilizes this information, is less clear (Dankiewicz *et al.*, 2002; Moore *et al.*, 1991; Roitblat *et al.*, 1991). Dependence of detection performance upon the number of available echoes has been demonstrated in the big brown bat (Surlykke, 1998).

Several theories exist regarding object detectability as a function of the number of observations available to a receiver. Dating back to the 1950's, several authors have investigated detection of multiple acoustic signals in noise. Green and Swets (1988) proposed two theories to account for the influence of multiple observations on signal detection performance. The first, termed the observation-integration model, assumes that the subject is able to retain information from successive presentations over a certain time period. Detectability is improved as long as the subject is able to successively integrate information from each stimulus presentation. The second model is based on threshold theory, and is comparable to the "multiple looks" model of temporal integration (Viemeister and Wakefield, 1991). In this model, each stimulus presentation can independently excite the sensory system. Given that the subject's momentary threshold varies with time, the likelihood of the stimulus exceeding the momentary threshold increases with the number of stimulus presentations.

Data obtained by Swets *et al.* (1964) and Swets and Green (1964) lend support to the integration model, and show that performance generally increases proportionally to the square root of the number of stimulus presentations. In a

[a)]Author to whom correspondence should be addressed. Electronic mail: altes@att.net

study examining the effect of multiple observations on sensory thresholds, Schafer and Shewmaker (1953) also found that thresholds decreased in proportion to the square root of the number of presentations. The integration model implies that the detectability index of a set of N presentations equals the square root of the sum-of-squares of the detectability indices for the individual presentations (Green and Swets, 1988). If the detectability indices for the individual presentations are identical, then the detectability index of a set of N presentations equals $\sqrt{N}$ times the detectability index of a single presentation. The $\sqrt{N}$ dependence follows from the definition of the detectability index, as given in the Appendix. Although many different integration models are possible (e.g., linear summation, energy detection, and binary summation), all such models have detectability indices that vary as $\sqrt{N}$.

Multiecho combining is relevant to many sonar capabilities, e.g., range-rate estimation and moving target indication (MTI) with short-duration, *Tursiops*-like waveforms, target tracking, and acoustic imaging in two or three dimensions. A logical step to investigate such capabilities in dolphins is to perform a critical experiment that ascertains whether the dolphin is capable of the simplest echo-combining task, which is to use multiple echoes from a stationary target to improve detection performance. If an accurate receiver model can be found, i.e., a model that accurately describes the dolphin's N-echo stationary-target detection performance, then this model may be applicable to more sophisticated dolphin echo-combining operations.

The current study was thus designed (i) to test the hypothesis that dolphins combine echoes to improve signal detectability; and (ii) to find the best receiver model to describe the dolphin's performance. A dolphin was trained to report detection of synthetic echoes generated by computer in response to the dolphin's clicks, placing the number of echoes available to the dolphin under experimental control. The dolphin's signal-detection performance was assessed when 1,2,4,8, and 16 echoes were made available. Although the available number of echoes (N) was preset, the dolphin's click emission rate was not controlled. The number of emitted dolphin clicks thus could be much larger than the number N of available echoes. During a test session, half of the trials contained synthetic echoes in noise and half contained noise only. Echo amplitudes were systematically decreased until detection fell to chance. At least two such thresholds were taken at each N level.

The results are summarized by plotting the signal-to-noise ratio (SNR) required for detection as a function of the number of available synthetic echoes that could be used by the dolphin. This experimental function is compared to the theoretical detection performance of three receiver models operating in additive, white, zero-mean Gaussian noise. All the receiver models initially are assumed to operate on one time sample (or range sample) from each available simulated echo, yielding N time samples altogether, where N is the number of available simulated echoes. The three models are linear summation, square-law summation (energy detection), and summation of binary-quantized sample values (binary M-out-of-N detection).

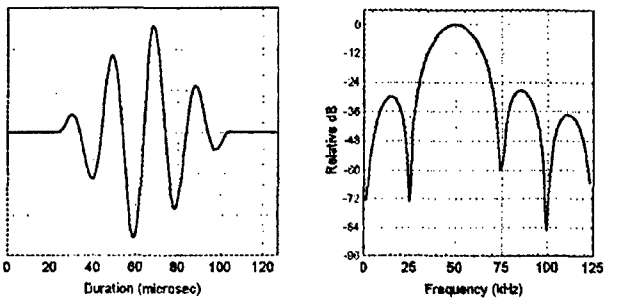

FIG. 1. Enlargement of GO stimulus pulse and corresponding spectrum. When more than one pulse was allowed per trial, pulse separation was constrained to be no smaller than 8 ms.

II. METHODS

A. Subject

The subject was a 17-year-old female Atlantic bottlenose dolphin (*Tursiops truncatus*; "CAS"). Floating pen enclosures on San Diego Bay, Space and Naval Warfare Systems Center were utilized for housing and experimental sessions. The subject resided with a small dolphin group but was separated from them when sessions were conducted. CAS' hearing was measured previously and shown to be normal (Brill *et al.*, 2001).

B. Synthetic echoes and noise

Conditions for behavioral responding were contingent upon two types of computer-generated stimuli. The NO-GO stimulus consisted of Gaussian noise with flat power spectrum over the echolocation bandwidth of the dolphin (95 dB SPL *re*: 1 μPa^2/Hz between 10 and 150 kHz). This white noise was present for the 4-s trial duration. The ambient noise in San Diego Bay had a power spectrum level decreasing from approximately 80 dB *re*: 1 μPa^2/Hz at 10 kHz to approximately 60 dB *re*: 1 μPa^2/Hz at 100 kHz, measured with one-octave spectrum analysis filters. The ambient noise level has increased with time and is thus larger than the level reported in Au (1993). The directivity of the dolphin's receiver (Au, 1993) further reduced the effective ambient noise level relative to the NO-GO stimulus. At 50 kHz, the ambient noise level was approximately 70 dB *re*: 1 μPa^2/Hz. This ambient noise level was 25 dB below the NO-GO stimulus level, and was 38 dB below the NO-GO stimulus level when the dolphin's directivity index is considered.

The GO stimulus included 1,2,4,8,16,32, or 64 pulses embedded in the white noise. The 32- and 64-pulse conditions were utilized during training phase sessions only. The number of pulses for GO stimulus trials did not vary within a session. Each pulse was a triangle-windowed 50-kHz 80-μs sinusoid (Fig. 1) delivered in response to the dolphin's outgoing echolocation click. An 8-ms click-pulse delay was inserted to simulate a 6-m range. The total range of the artificial echoes was 7m, counting propagation time between the transducers and the dolphin. Although the dolphin's click emission rate was not experimentally controlled, it was influenced by this imposed range parameter (Penner, 1988). Pulse source level was manipulated to determine CAS' de-

tection thresholds above the noise floor. No attempt was made to associate or equate the artificial stimuli with echoes encountered under nonexperimental conditions.

C. Apparatus

Synthetic echoes were generated and delivered by an electronic synthetic echo system (SES). One electronic echo was delivered for every click emitted by the subject up to the maximum N allowed for that session per trial. The dolphin's clicks were detected by a Reson TC4013 hydrophone located 0.64 m directly in front of her melon and triggered a single electronic echo if the received level exceeded 170 dB *re*: 1 μPa. Clicks were bandpass filtered (3–300 kHz) and amplified by 54 dB before reaching a multifunction board (National Instruments PCI MIO-16E-1; on Pentium PC) where triggering of synthetic echoes previously stored to RAM occurred. Upon receiving a trigger, the SES converted a digital waveform to an analog signal that was then filtered (10–200 kHz) and amplified (20 dB) by a DL Electronics 4302 filter/amplifier. Analog echoes were added to the white noise using custom hardware and projected to the subject by a second TC4013 hydrophone located 0.7 m beyond the trigger hydrophone. The echo stimulus thus emanated from a transducer that was 1.34 m from the dolphin's melon, located on a horizontal line directly in front of the melon. A 7-m echo range was simulated by insertion of an 8-ms delay between the trigger event and output of an echo (12-m electronic delay plus 2-m propagation delay, divided by 2). System calibration included SPL measurements of TC4013 electronic echo projection by an ITC 6030 omnidirectional hydrophone located at the subject's test station position. Surface reflections were absorbed and dispersed by a cluster of nylon-bristle brushes placed at the water surface midway between the dolphin and the transducers.

D. Session procedure

CAS was positioned at an intertrial station in front of an experimenter before a trial. At the start of each trial, CAS was cued to submerge into a test station hoop 1.35 m below the water surface by the experimenter's hand gesture. An acoustically opaque screen (a PVC sheet covered with closed-cell foam neoprene) placed in front of the hoop was removed and the SES simultaneously activated, initiating white noise and permitting the dolphin to begin echolocating. The 4-s white-noise burst defined the trial duration for the dolphin. To report a signal-present condition (GO response), the dolphin immediately moved to a nearby paddle and touched it with her rostrum. To indicate the absence of a signal (NO-GO response), she remained stationary in the hoop for the trial duration (4 s). If CAS did not begin movement toward the paddle before the end of the 4-s window, her response was classified as NO-GO. CAS typically initiated a GO response within 1–2 s. Tone and fish rewards were given for every correct response. An equal number of GO and NO-GO trials was presented in a randomized Gellermann series (Gellermann, 1933). The likelihood of a GO following a NO-GO (or the reverse) followed a 0.5 first-order conditional probability for every ten-trial block. The dolphin's motivation to perform reliably was assessed by ten warm-up trials before every session, with an 80%-correct response rate required in order for a test session to ensue. No more than one experimental session was conducted in a day.

E. Threshold titration

Thresholds were estimated for both training and testing phases by using a signal amplitude titration method (up/down staircase) that was contingent upon the dolphin's responses to GO stimulus trials (Moore and Schusterman, 1987). During the sessions, the experimenter manipulated SPL by changing the voltage value of the synthetic echo amplitude. Initially, GO signal amplitude was held constant and easily discernible for the first ten trials of the session. After the first ten trials, 0.2-V decrements in signal amplitude were made until the dolphin responded incorrectly. Amplitude was raised in 0.1-V increments until the dolphin detected the signal again. All subsequent amplitude adjustments were in 0.1-V steps, with decrements made after every correct GO response and increases after every incorrect response. A change in direction of amplitude adjustment constituted a reversal, and a threshold estimate was taken after ten reversals were acquired by calculating the mean decibel level at those reversal points (50%-correct detection rate). As CAS became experienced with the task, and echo amplitudes were close to the white-noise floor, the titration deltas were changed to 0.05 V. Logarithmic steps (constant $\Delta v/v$) are more compatible with an animal's sensitivity to differences than constant Δv steps, but constant steps are approximately proportional to logarithmic steps when the steps are small relative to the threshold level ($\Delta v \ll v$).

F. Animal training

Training the stimulus-response contingency was accomplished by imposing minimal restrictions on the GO stimulus variables in an effort to highlight differences from the NO-GO stimulus. A generous number of synthetic echoes were provided ($N=256$) and signal amplitude was held approximately 40 dB above the noise floor (1.0 V). Stimuli were presented in three to six same-trial blocks, e.g., four NO-GO trials followed by six GO trials. Approximately four sessions were required before the appropriate responding was observed. Trial type was then randomized as described previously. Once responding was stable, CAS was introduced to a reduction in N. One to eight sessions (s) were conducted at successively lower N levels as follows: $N=64$ ($s=8$); $N=32$ ($s=3$); $N=16$ ($s=5$); $N=8$ ($s=1$); $N=4$ ($s=5$); $N=2$ ($s=2$); and $N=1$ ($s=3$). Thresholds were estimated during the final three sessions at $N=64$, 16, 4, and 1, and during the final session only at $N=32$, 8, and 2. Once CAS demonstrated stable performance at the minimum N level ($N=1$), as indicated by the threshold session results at $N=1$, no further training was undertaken.

G. Testing

Exposure to all experimental conditions was completed in the training phase so that testing-phase thresholds were free of novelty effects. Two ($N=1,4,8,16$) or three ($N=2$)

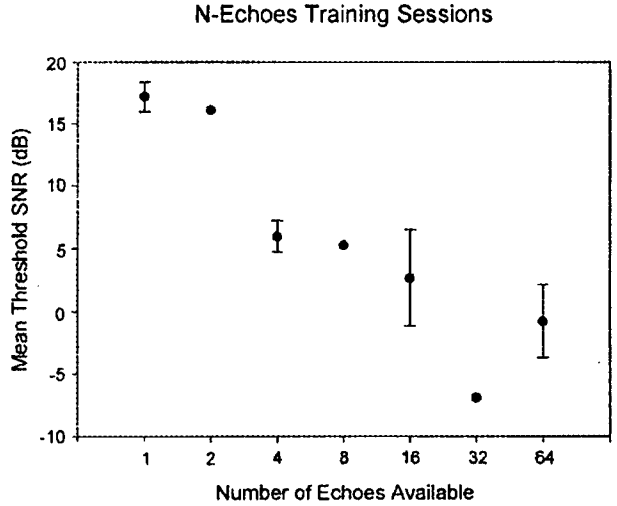

FIG. 2. Average detection threshold in decibels obtained during training sessions when the number of available echoes per trial (N) was 1, 4, 16, 64 (number of measured thresholds =3) or 2, 8, 32 (number of measured thresholds = 1). Error bars for the trials with three measured thresholds represent SEM (standard error of the mean).

final thresholds were obtained in which signal detection performance as a function of N was assessed. N was held constant during a session while signal amplitude was titrated as described previously.

H. Calculating thresholds

Recall that the experimenter manipulated SPL by changing the voltage value of the synthetic echo amplitude. Synthesized white, Gaussian noise was held constant at 95 dB *re*: 1 μPa^2/Hz. Thresholds were computed as signal-to-noise ratios (SNR), the required echo amplitudes $A(N)$ for detection with N available echoes, divided by the rms noise power. The bandwidth for rms noise power was estimated using Q derived from critical band measures of the bottlenose dolphin receiver. Q was approximately 2.2 for signals with center frequency of 60 kHz (Au and Moore, 1990). The synthetic signals used in this study had center frequency of 50 kHz; thus, noise bandwidth was estimated to be approximately 22.72 kHz. The calibrated system permitted conversion of the voltages $A(N)$ to dB, thereby allowing computation of SNR in dB by subtracting rms noise power (dB) from synthetic echo amplitude $A(N)$ (dB). Importantly, note that SNR was computed *per echo*, without weighting for the number of available echoes N.

III. RESULTS

A. Animal training

Figure 2 shows results of the initial detection threshold sessions that were conducted at each N level. N is presented on the horizontal axis, with sessions represented left-to-right in the opposite order in which they were conducted. Detection performance was strong for N values of 64, 32, and 16, although sporadic threshold elevations were seen. It is likely that these variations represent CAS' growing familiarization with the manipulation of N while the thresholds were being

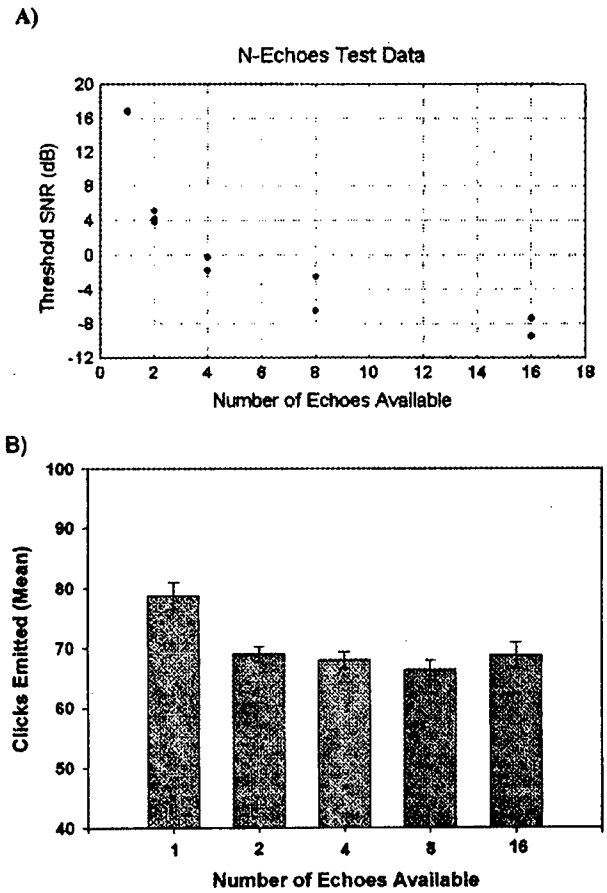

FIG. 3. Test session data: (A) Final detection thresholds in decibels when the number of available echoes per trial (N) was 1, 4, 8, 16 (number of measured thresholds = 2) or 2 (number of measured thresholds =3). The two measured thresholds at N= 1 were equal and the dots at N = 1 therefore overlap. (B) Average number of clicks emitted per trial at each N level (pooled sessions). Error bars represent SEM. Significantly more clicks were emitted at N= 1 compared to all other levels (Tukey–Kramer, α=0.05).

titrated. At N values of 8 and 4, SNR required for detection increased, and was highest when N was held at 2 and 1. The mean false-alarm rate for the threshold sessions was 0.088 (s.d.=0.069). Click emission was tracked for every trial and results showed that CAS always emitted enough clicks to receive the maximum number of echoes that were allowed (mean clicks per trial=80).

B. Threshold testing

The top panel of Fig. 3 summarizes CAS' detection thresholds that were estimated during the test phase of the experiment. N is presented on the horizontal axis, with successive sessions represented in left-to-right order. The two estimated threshold SNR values for N= 1 were identical, and are thus represented by a single point in Fig. 3. Detection thresholds were lower overall at each N level when compared to the training session thresholds, perhaps due to increased familiarization with the task. Mean false-alarm rate was 0.034 (s.d.=0.042). The thresholds are well behaved, with SNR required for detection falling off monotonically as the number of echoes (N) is increased. Recall that SNR is

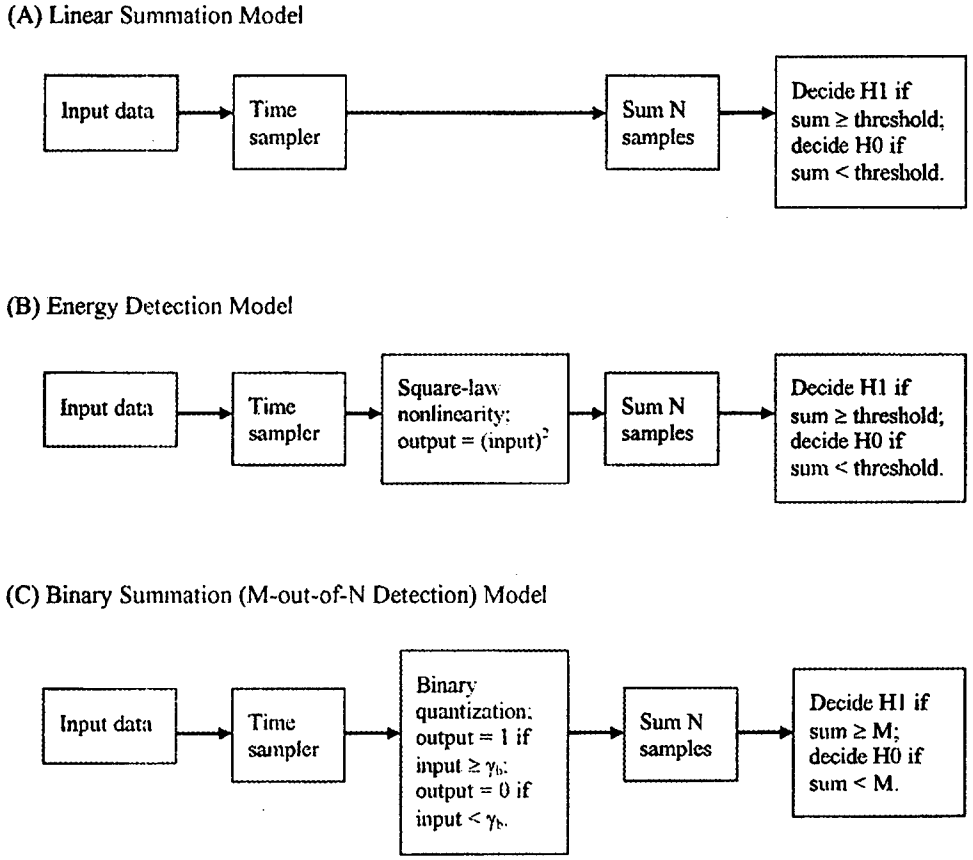

FIG. 4. Receiver models that are compared with dolphin N-echo detection data. (A) linear summation; (B) energy detection; (C) binary summation (M-out-of-N detection). H1 is the signal-plus-noise hypothesis corresponding to the GO stimulus. H0 is the noise-only hypothesis corresponding to the NO-GO stimulus.

measured per echo. The trend is consistent with those from human listeners showing that detection improved as the number of signals was increased (Green and Swets, 1988; Swets and Green, 1964). These results support the inference that CAS was able to combine multiple echoes in her biological signal-processing system.

The lower panel of Fig. 3 summarizes the distribution of clicks emitted by CAS that were above 170 dB during each session. Analysis by a one-way ANOVA showed a difference in click production as a function of N, $F(4,524)=5.4$, $p<0.0003$. Comparison among the means using the Tukey–Kramer test revealed that CAS emitted significantly more clicks for the $N=1$ condition than all the others ($\alpha=0.05$, two-tail), supporting the notion that this condition was more difficult than $N=2$, 4, 8, and 16. Further evidence for difficulty at $N=1$ is that the change in threshold for the $N=1$ condition compared to the $N=2$ condition was 12 dB, whereas the change in threshold between the other conditions ($N=2$ through $N=16$) was almost a consistent 4-dB change. The mean number of clicks emitted during all testing sessions was 70, only a slight decrease from the average number emitted during training sessions. CAS always emitted more clicks than echoes that were available, thus ensuring that she received all available synthetic echoes.

C. Receiver models

Various models of animal echolocation have been employed to understand the signal-processing operations that may be used by the animals and to guide the design of broadband sonar systems that attempt to emulate animal capabilities. Receiver models that incorporate summation or integration are relevant to this inquiry. Well-known integration models pertain to summation over intervals in range/delay/time (critical intervals; Vel'min and Dubrovskiy, 1976) and over intervals in frequency (critical bands; Johnson, 1968). The synthetic echo in Fig. 1 fits within a single critical interval and a single critical band for a critical bandwidth of 22.72 kHz at a frequency of 50 kHz (Au and Moore, 1990). This study addresses integration along a different dimension, correspnding to the number of click–echo pairs (Floyd, 1980; Surlykke, 2003). A critical N value, corresponding to the maximum number of echoes that can be integrated by the dolphin, has yet to be determined. Figure 3 implies that the critical N is greater than 16.

Three integration models are considered here in order to better understand the SNR required by a dolphin for target detection when the number of available echoes is varied. These models correspond to linear summation, energy detection, and summation of binary-quantized echo data (binary M-out-of-N detection). The operations performed by the three models are illustrated in Fig. 4.

The N-echo detection performance of the three receivers is predicted by the analysis in the Appendix. For the linear summation, energy detection, and binary M-out-of-N receivers, the required echo amplitudes $A(N)$ for detection with N

available echoes, divided by the rms noise power σ, are

$$[A(N)/\sigma]_{\text{lin}}=c_l/\sqrt{N}, \tag{1}$$

$$[A(N)/\sigma]_{\text{cgy}}=(c_e/\sqrt{N})[1+\sqrt{1+(2N/c_e^2)}]^{1/2}, \tag{2}$$

$$[A(N)/\sigma]_{\text{bin}}=\text{erfc}_*^{-1}(p_0)-\text{erfc}_*^{-1}(p_1), \tag{3}$$

where c_l and c_e are constants, $\text{erfc}_*^{-1}(\cdot)$ is the inverse complementary error function (Fig. 5), p_0 is the probability that the threshold level of the binary quantizer is exceeded when only noise is present (the H0 hypothesis), and p_1 is the probability that the binary quantizer threshold is exceeded when both signal and noise are present (the H1 hypothesis). The function $\text{erfc}_*^{-1}(p)$ is related to the probit transformation (Collett, 1952),

$$\text{erfc}_*^{-1}(p)=\text{probit}(1-p). \tag{4}$$

In the binary summation model, probability p_1 depends upon p_0, N, and a constant c_b

$$p_1=\frac{(2p_0+c_b/N)+\sqrt{(2p_0+c_b/N)^2-4p_0(1+c_b/N)[p_0(1+c_b/N)-c_b/N]}}{2(1+c_b/N)}. \tag{5}$$

For a prespecified value of p_0, all the $A(N)/\sigma$ expressions in (1)–(3) depend on a constant (c_l, c_e, or c_b) and on the number of available echoes, N.

D. Comparison of theoretical performance with dolphin data

To compare the receiver models with dolphin detection data, the parameters c_l, c_e, p_0, and c_b are adjusted to provide a minimum mean-square error (MMSE) fit between the values of $[A(N)/\sigma]_{\text{model}}$ in (1)–(4) and the average experimental value of $A(N)/\sigma$ for each N value. The correlation coefficients between the average data points and their theoretical counterparts are computed for each model. For visual comparison, the data points and theoretical curves are plotted together in Fig. 6 on a decibel scale, showing $20\log_{10}[A(N)/\sigma]$ vs N. Figure 6 illustrates that the best fit (by far) is obtained with the binary M-out-of-N receiver.

The best-fit parameters and data-model correlation coefficients r are as follows:

Linear summation model: $c_l=4.58$, $r_l=0.9055$, (6)

Energy detection model: $c_e=3.12$, $r_e=0.9095$, (7)

Binary M-out-of-N detection:

$$p_0=0.5,\ c_b=0.999\,999\,3,\ r_b=0.9997. \tag{8}$$

The more accurate specification of c_b is necessitated by receiver operation on a steep part of the curve in Fig. 5 when $N=1$, as discussed in the Appendix.

The binary M-out-of-N detector seems to have an unfair advantage because two parameters can be varied instead of one, providing an extra degree of freedom for data fitting. The extra degree of freedom is eliminated by choosing a prior value for p_0. Choosing a fixed p_0 value is equivalent to choosing a threshold for binary quantization. The most appropriate prior choice for the binary quantization threshold is zero, which implies that $p_0=0.5$ for all symmetric, zero-mean noise distributions, independent of the noise power σ^2.

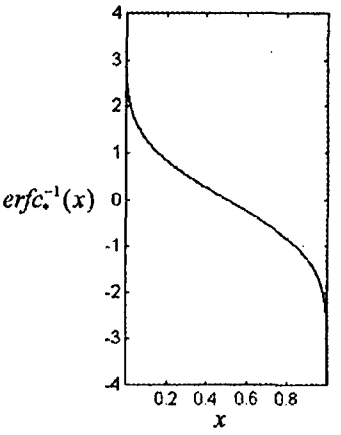

FIG. 5. The inverse complementary error function $\text{erfc}_*^{-1}(x)$.

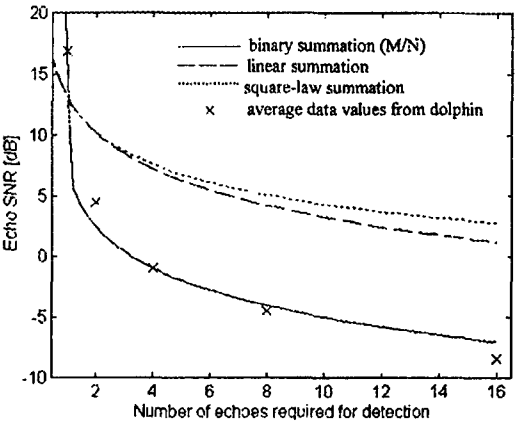

FIG. 6. MMSE (minimum mean-square error) fits between three receiver models and dolphin N-echo detection data. The MMSE algorithm compares models to noise-normalized data amplitudes $A(N)/\sigma$, but the curves are shown on a dB scale corresponding to $\text{SNR[dB]}=20\log_{10}[A(N)/\sigma]$.

Variation of p_0 can be used to check the results, since the best p_0 value for nonparametric operation is known to be 0.5.

IV. DISCUSSION

A. Estimation of detectability index

The analysis in the Appendix indicates that the constants c_l, c_e, and c_b are related to the corresponding detectability indices by the equations

$$c_l = d_l; \quad c_e = d_e; \quad c_b = d_b^2/2. \tag{9}$$

The detectability indices corresponding to the MMSE estimates of c_l, c_e, and c_b are

$$d_l = 4.58; \quad d_e = 3.12; \quad d_b = 1.41, \tag{10}$$

for the linear summation, energy detection, and binary M-out-of-N receivers, respectively. These performance measures are based on a restricted set of N values equal to 1, 2, 4, 8, and 16. The receiver model with the best fit to the data has the worst performance in zero-mean Gaussian noise.

B. Distribution tolerance of the binary summation model

The linear receiver is optimum for Gaussian noise with known variance, but the binary M-out-of-N processor has distribution-tolerant (nonparametric) properties. The false-alarm rate of the binary M-out-of-N receiver is insensitive to time-varying noise power and to the shape of any symmetric, zero-mean noise distribution. If the binary M-out-of-N receiver is a viable model for dolphin multiecho processing, then the dolphin has traded optimality in Gaussian noise with specified noise power for robustness with respect to the distribution and power of the noise. The performance disparity between binary and linear summation is not large if many echoes are used. Figure 6 implies that large N is associated with small SNR for all of the models. For large N and small SNR, it is shown in the Appendix that $d_l \approx 1.25 d_b$.

C. Preprocessing with an auditory transduction model

Figure 6 illustrates the performance of an M-out-of-N receiver with zero binary quantization threshold. This performance is unaffected by preprocessing input data with a sign-preserving zero-memory nonlinear transformation. Two examples of such a transformation are (1) a half-wave rectifier and (2) membrane potential as a function of the displacement of either inner or outer hair cells (Russell *et al.*, 1986; Mountain and Hubbard, 1996). The binary summation model is insensitive to the nonlinear signal transformation that occurs during cochlear transduction from acoustic waveforms to neuronal excitations.

An envelope preprocessor is approximated by a weighted average of neighboring half-wave rectified data samples. A receiver model that uses envelope detection prior to binary quantization and M-out-of-N detection cannot be ruled out with current data.

D. Phase sensitivity

Phase sensitivity of the dolphin N-echo receiver model is still an open question. If the data are linearly processed, half-wave rectified, or passed through a zero-memory hair cell model before binary quantization, then phase sensitivity depends upon maintaining an accurate sampling time relative to the time of signal transmission. Multiple, parallel M-out-of-N detectors can be used to test hypothesized sampling times, to compensate for sampling time errors, and to generate range-tracking information. If an envelope detector that forms a weighted sum of neighboring half-wave rectifier outputs is used as a preprocessor, then receiver tolerance to sampling time errors is increased but phase sensitivity is reduced.

To test phase sensitivity, the waveform in Fig. 1 can be replaced with a signal that has a short-duration, high-amplitude positive peak followed by (or surrounded by) long-duration, small-amplitude negative components with the same total area as the positive peak. Phase reversal of this waveform (multiplication by -1) should affect the detection performance of a phase-sensitive receiver.

E. Postdetection integration

The binary M-out-of-N receiver model is equivalent to a postprocessor for a detector that makes an H1 versus H0 decision at each range sample, for each click–echo pair. The binary decision variable at a given range is integrated or counted over successive click-echo pairs. A different strategy is followed by the linear and quadratic summation models, which do not implement a decision until all relevant data are summed. The latter strategy is generally regarded as superior because the level of each detector output is preserved and no information is lost via premature decision making. A large transient interference pulse (e.g., from a snapping shrimp), however, will have a much larger effect on linear or quadratic summation than upon summation of binary decision variables (Bullock, 1986). In San Diego Bay and many other locations, snapping shrimp are an important source of interference for dolphin echolocation (Au and Banks, 1998). Aside from interference considerations, the dynamic range tolerance provided by binary quantization may be important for detection, tracking, and acoustic imaging of prey with large aspect-dependent variation in target strength.

F. Biological neural networks

The binary M-out-of-N detector model is a basic building block for neural networks that process action potentials, which are binary, all-or-none signals. A neuronal version of a binary M-out-of-N processor could use binary sampling intervals corresponding to the width of an action potential spike. If the intensity of a stimulus is encoded by the density of action potential spikes and/or the duration of a spike sequence, the binary M-out-of-N processor can function as a stimulus intensity or amplitude decoder, despite the amplitude insensitivity associated with binary quantization.

G. Polarity coincidence correlation and binaural localization models

The binary M-out-of-N detector is a polarity coincidence correlator with a constant, unit reference function. The polarity coincidence correlator is well known for its relative insensitivity to the probability distribution of input data (Wolff *et al.*, 1962). A neurophysiological model for binaural localization (interaural time delay estimation) uses coincidence of the excitations in two neural delay lines, one from each ear (Jeffress, 1948; Konishi, 1993; Colburn, 1996). This binaural model is similar to polarity coincidence correlation and thus to the binary M-out-of-N receiver model. In biological sonar systems, interaural polarity coincidence correlation can be used for azimuth estimation (and for elevation estimation if the animal rolls by 90 degrees). Range tracking can be implemented via cross correlation of successive echoes, using a polarity coincidence correlator.

H. Binary quantization and zero crossings

A binary waveform representation preserves information about real zero crossings, which are important signal attributes (Kedem, 1994; Marr, 1982; Requicha, 1980; Voelcker, 1966a, 1966b). A polarity coincidence correlator can use these attributes for detection, estimation, classification, and decomposition via Haar functions (Hagen and Farley, 1973; Vetterli and Kovacevic, 1995).

I. Capabilities of a multipulse sonar receiver that uses binary summation

The ability of a dolphin to combine information from multiple pulse–echo pairs is necessary for advanced signal-processing capabilities. One of these capabilities is acoustic imaging via a simplified version of synthetic aperture sonar (SAS) processing (Altes, 1995; Altes *et al.*, 1998; Altes, 2003). SAS images can be formed by adding the echo sample at each range to an appropriate pixel in a two- or three-dimensional image. The image is sequentially constructed as multiple echoes are obtained from different aspects. High-resolution SAS images have been created from binary-quantized sonar echo envelopes (with a nonzero quantization threshold), using dolphin-like transmitted waveforms (Altes, personal observation). After N echoes are processed, each pixel level in such an image represents the response of a binary M-out-of-N receiver.

The dolphin may use multipulse processing to estimate range-rate, implement a moving target indicator (MTI), track targets, and perform acoustic imaging in two or three dimensions. Figure 6 implies that the dolphin can perform robust integration along a constant-range line in the range, echo-number (R,N) plane. Range-rate estimation, tracking, and acoustic imaging involve integration along other lines or curves in the R,N plane. The simplest moving target indicator computes the difference between successive detector outputs along a constant-range line in the R,N plane. A more sophisticated MTI uses a weighted sum of such outputs, with positive and negative weights.

J. Adaptability of the dolphin receiver

The power spectrum of artificially added Gaussian noise (white over the dolphin's echolocation bandwidth) was 95 dB *re*: 1 μPa^2/Hz. When an extra 13 dB is added to account for the dolphin's directivity index, the artificial Gaussian noise was 108 dB above spatially uniform noise with a power spectral density of 1 μPa^2/Hz, and 38 dB above the average ambient noise level of 70 dB *re*: 1 μPa^2/Hz. The ambient level included average snapping shrimp interference and the sounds of other dolphins in the area. Despite the 38-dB difference, the analysis indicates that the dolphin's receiver did not adapt to operation in Gaussian noise as opposed to strong transient interference. This apparent lack of adaptability can be explained by the large disparity between peak and average levels of transient sounds. At a distance of 1 meter, the power spectral density of a single snapping shrimp pulse is between 105 and 111 dB *re*: 1 μPa^2/Hz (Au and Banks, 1998; Versluis *et al.*, 2000). Spherical spreading decreases this level by 20 log r if the shrimp is r meters from the receiver. A spatially averaged interference power spectral density level of 108 dB *re*: 1 μPa^2/Hz is required to make the interference power spectrum equal to the power spectrum of the artificially added Gaussian noise at the input to the dolphin's receiver. The possible presence of nearby snapping shrimp thus could have constrained the dolphin's receiver design. The experiment was performed in an area with floating walkways to support trainers and equipment. Snapping shrimp appear to congregate in such areas (Ferguson and Cleary, 2001).

V. CONCLUSION

Synthetic echoes in additive noise were used to estimate the SNR required by a dolphin for detection when the number of available echoes was varied. A close fit to the dolphin's performance data was obtained with a receiver model that sums binary-quantized time samples from N available echoes. This detector does not perform as well as linear summation for Gaussian noise with known average power, but its false-alarm rate is distribution tolerant and nonparametric with respect to variable noise power. The dolphin's acoustic environment is, in fact, notoriously non-Gaussian and nonstationary (Urick, 1975). The close fit of the binary M-out-of-N model to the dolphin detection data, together with the relatively poor fit of the linear and energy summation models, implies that the dolphin trades optimality (in Gaussian noise with known power) for robustness.

Further experiments are needed to determine whether the dolphin's time sampling is sufficiently precise to allow phase sensitivity in the context of the binary summation model. Even without phase sensitivity, binary summation can be used for acoustic imaging. Binary M-out-of-N detection is a special case of polarity coincidence correlation (a model for binaural localization), and it is similar to operations performed by biological neural networks. Another question is whether the dolphin's receiver can adapt to optimum operation in Gaussian noise when snapping shrimp are not present.

ACKNOWLEDGMENTS

We thank Justine M. Zafran and Michael D. Massimi for their assistance during the behavioral data collection phase of this study. This research was made possible in part thanks to support from Dr. John Tague and Dr. Robert Gisiner (Office of Naval Research 321US and 342). Helpful critiques were provided by Dr. Magnus Wahlberg (Department of Zoophysiology, Aarhus University, Denmark) and Dr. David Kastak (University of California at Santa Cruz).

APPENDIX: DETECTABILITY INDEX DERIVATIONS

The output mean values and variances from each receiver model in Fig. 4 can be used to predict the detectability index at the receiver output. The detectability index is closely related to the Fisher ratio and to the t-statistic. Receiver performance (detection, false alarm, and error probabilities) can be computed from the detectability index if the output distributions are Gaussian with equal variance under noise-only and signal-plus-noise conditions (Van Trees, 1968). This condition seldom applies to nonlinear receivers. Detection performance, however, almost always varies monotonically with the detectability index, which is defined as the difference between the output mean value when hypothesis H1 (signal plus noise) is true and the output mean value when H0 (noise alone) is true, divided by the square root of the average output variance for the two hypotheses.

Addition of N independent receiver outputs with fixed SNR causes the mean output and variance to be multiplied by N, for both H1 and H0. The detectability index for the sum is then the detectability index for a single observation multiplied by the square root of N. Equivalently, the detectability index of the sum is the square root of the sum-of-squares of the detectability indices for the individual observations as in Green and Swets (1988), regardless of the receiver model, for constant SNR.

In the following analysis, the detectability index of each receiver model is assumed to vary monotonically with detection performance and to be constant for all values of N, the number of echoes available for detection. A constant detectability index for all N values implies that SNR decreases with N. These assumptions imply that each receiver model (as well as the dolphin) uses a consistent performance criterion (detection, false alarm, and error probability) for decision making at all N values.

Since the detectability index d depends upon SNR and N, it should be possible to obtain an expression for SNR $=20\log[A(N)/\sigma]$ as a function of d and N. The noise-normalized echo amplitude required for detection, $A(N)/\sigma$, depends upon the detectability index d and the number of available echoes N. For the binary summation model, $A(N)/\sigma$ also depends upon the threshold γ_b for binary quantization, or equivalently, on the probability p_0 of a threshold crossing when H0 is true. In general

$$[A(N)/\sigma]_{\text{theory}}=f_{\text{rcvr}}(d,N,\gamma_b), \tag{A1}$$

where the function $f_{\text{rcvr}}(d,N,\gamma_b)$ depends upon the receiver model.

The experimental results yield the average signal-to-noise ratio (SNR) in decibels at specific N values, and

$$[A(N)/\sigma]_{\text{expt}}=10^{\text{SNR}/20}. \tag{A2}$$

For each receiver model, a gradient descent algorithm is used to find the value of d (and p_0 or γ_b if one of these quantities is not prespecified) that minimizes the mean-square difference between $[A(N)/\sigma]_{\text{theory}}$ and $[A(N)/\sigma]_{\text{expt}}$ at the N values that were used in the experiment. The resemblance between a model and the experimental data is quantitatively represented by a correlation coefficient (Hays, 1994) computed from the $A(N)/\sigma$ values of the best-fit model and the data at the experimental N values.

The linear summation model computes the function

$$h(\underline{x})=(1/N)\sum_{i=1}^{N}(x_i+A), \tag{A3}$$

where A is the sampled signal value and $\{x_i;i=1,...,N\}$ are independent identically distributed noise samples (one from each echo) with zero mean and variance σ^2; $E(x_i)=0$ and $E(x_ix_j)=\sigma^2$ if $x_i=x_j$, and zero otherwise. $E(x)$ is the ensemble expected value of x, and $\underline{x}$ is the set of noise samples $x_1,x_2,\ldots,x_N$. It follows that

$$E[h(\underline{x})]=(1/N)\sum_{i=1}^{N}E(x_i+A)=A, \tag{A4}$$

and

$$\begin{aligned}E[h^2(\underline{x})]&=(1/N^2)\sum_{i=1}^{N}\sum_{j=1}^{N}E[(x_i+A)(x_j+A)]\\&=(1/N^2)\left[\sum_{i=1}^{N}E[(x_i+A)^2]\right.\\&\quad\left.+\sum_{i=1}^{N}\sum_{j\neq i}E[(x_i+A)(x_j+A)]\right]\\&=(\sigma^2/N)+A^2.\end{aligned} \tag{A5}$$

The variance of the averaged, linearly transformed data is then

$$\text{Var}[h(\underline{x})]=E[h^2(\underline{x})]-E^2[h(\underline{x})]=\sigma^2/N. \tag{A6}$$

When hypothesis H1 is true, the data consist of signal plus noise with $A\neq 0$. If H0 is true, the data consist of noise alone ($A=0$). The corresponding detectability index is

$$\begin{aligned}d_l&=\frac{|E[h(\underline{x})|H1]-E[h(\underline{x})|H0]|}{[(1/2)\{\text{Var}[h(\underline{x})|H0]+\text{Var}[h(\underline{x})|H1]\}]^{1/2}}\\&=\sqrt{N}A/\sigma.\end{aligned} \tag{A7}$$

In the psychophysical literature, d' is used instead of d. The prime is omitted here in order to simplify notation in the equations.

The linear summation model is evaluated by adjusting the constant $c_l=d_l$ in the equation

$$[A(N)/\sigma]_{\text{lin}}=c_l/\sqrt{N}, \tag{A8}$$

to obtain a minimum mean-square error (MMSE) fit of $[A(N)/\sigma]_{\text{lin}}$ to $[A(N)/\sigma]_{\text{expt}}$ for the experimental values of N. The resulting best fit is then evaluated via the correlation coefficient between $[A(N)/\sigma]_{\text{lin}}$ and $[A(N)/\sigma]_{\text{expt}}$.

For an average of squared data samples (energy detection)

$$h(\underline{x})=(1/N)\sum_{i=1}^{N}(x_i+A)^2, \tag{A9}$$

$$E[h(\underline{x})]=(1/N)\sum_{i=1}^{N}E(x_i+A)^2=\sigma^2+A^2, \tag{A10}$$

and

$$E[h^2(\underline{x})]=(1/N^2)\sum_{i=1}^{N}\sum_{j=1}^{N}E[(x_i+A)^2(x_j+A)^2]$$

$$=(1/N^2)\left[\sum_{i=1}^{N}E[(x_i+A)^4]+\sum_{i=1}^{N}\sum_{j\neq i}E[(x_i+A)^2(x_j+A)^2]\right], \tag{A11}$$

where

$$E[(x_i+A)^4]=E(x_i^4)+4E(x_i^3)A+6E(x_i^2)A^2+4E(x_i)A^3+A^4. \tag{A12}$$

For a zero-mean Gaussian random variable, $E(x_i)=0$, $E(x_i^2)=\sigma^2$, $E(x_i^3)=0$, and $E(x_i^4)=3\sigma^4$. It follows that

$$E[h^2(\underline{x})]=(1/N)(3\sigma^4+6\sigma^2A^2+A^4)+[(N-1)/N](\sigma^2+A^2)^2, \tag{A13}$$

and

$$\text{Var}[h(\underline{x})]=E[h^2(\underline{x})]-E^2[h(\underline{x})]=(2\sigma^2/N)(\sigma^2+2A^2). \tag{A14}$$

The detectability index is then

$$d_e=\frac{|E[h(\underline{x})|H1]-E[h(\underline{x})|H0]|}{[(1/2)\{\text{Var}[h(\underline{x})|H0]+\text{Var}[h(\underline{x})|H1]\}]^{1/2}}$$

$$=\sqrt{N/2}\frac{(A/\sigma)^2}{\sqrt{1+(A/\sigma)^2}}$$

$$\cong\sqrt{N/2}|A/\sigma| \text{ at high SNR } (|A/\sigma|\gg 1)$$

$$\cong\sqrt{N/2}(A/\sigma)^2 \text{ at low SNR } (|A/\sigma\ll 1). \tag{A15}$$

For a general square-law model with no assumptions about SNR, the first equation in (A15) can be written

$$(N/2)x^2-d_e^2x-d_e^2=0, \tag{A16}$$

where $x=(A/\sigma)^2$. Solving for x yields

$$A(N)/\sigma=[(d_e^2/N)\pm(d_e/N)\sqrt{d_e^2+2N}]^{1/2}. \tag{A17}$$

To obtain a real-valued $A(N)/\sigma$, the plus-or-minus operation in (A17) must always be plus, and

$$[A(N)/\sigma]_{\text{cgy}}=(c_e/\sqrt{N})[1+\sqrt{1+2(c_e/\sqrt{N})^{-2}}]^{1/2}, \tag{A18}$$

where $c_e=d_e$. To evaluate the general square-law model, the constant c_e in (A18) is adjusted to obtain an MMSE fit of $[A(N)/\sigma]_{\text{cgy}}$ to $[A(N)/\sigma]_{\text{expt}}$ for the experimental values of N.

For the M-out-of-N receiver model, the binomial distribution (Papoulis, 1965) describes the probabilities of various numbers of ones and zeros at the output of the binary quantizer for N echoes. Let p_1 equal the probability that the binary random variable equals 1 (the sampled data value is greater than the binary quantization threshold, γ_b) when an echo is present (the signal plus noise condition, H1). Let p_0 equal the probability that the binary random variable is 1 when the echo is absent (the noise alone condition, H0). For one binary sample from each of N echoes

The expected number of "ones" with echo present (H1) equals Np_1.
The expected number of "ones" with echo absent (H0) equals Np_0.
The variance of the distribution of the number of "ones" given H1 equals $Np_1(1-p_1)$.
The variance of the distribution of the number of "ones" given H0 equals $Np_0(1-p_0)$.

The detectability index is the difference in means divided by the square root of the average variance.

$$d_b=\frac{Np_1-Np_0}{\sqrt{(1/2)[Np_1(1-p_1)+Np_0(1-p_0)]}}. \tag{A19}$$

As in the previous models described by (A8) and (A15), the detectability index is proportional to the square root of N if p_1 is constant (constant SNR).

If a threshold value γ_b is used to convert echo samples into binary data, the probability that the binary random variable equals 1 when the signal is absent (noise alone) is

$$p_0=\text{erfc}_*(\gamma/\sigma), \tag{A20}$$

and the probability that the binary random variable equals 1 when the signal is present is

$$p_1=\text{erfc}_*\{[\gamma-A(N)]/\sigma\}, \tag{A21}$$

where σ is the rms noise power and the complementary error function $\text{erfc}_*(x)$ is the integral of a zero-mean, unit variance normal distribution between x and infinity.

From (A20), the threshold level is

$$\gamma=\sigma\,\text{erfc}_*^{-1}(p_0), \tag{A22}$$

where $\text{erfc}_*^{-1}(p_0)$ is the inverse complementary error function of p_0 as in Fig. 5. Similarly, (A21) can be solved for $A(N)$:

$$A(N)=\gamma-\sigma\,\mathrm{erfc}_*^{-1}(p_1). \tag{A23}$$

Substituting (A22) into (A23),

$$[A(N)/\sigma]_{\mathrm{bin}}=\mathrm{erfc}_*^{-1}(p_0)-\mathrm{erfc}_*^{-1}(p_1). \tag{A24}$$

Letting $c_b=(1/2)d_b^2$ and solving (A19) for p_1 yields

$$p_1=\frac{(2p_0+c_b/N)\pm\sqrt{(2p_0+c_b/N)^2-4p_0(1+c_b/N)[p_0(1+c_b/N)-c_b/N]}}{2(1+c_b/N)}. \tag{A25}$$

The plus-or-minus operation in (A25) must always be plus in order for p_1 to be non-negative. For a given level of detection performance (e.g., a given percentage of correct decisions), the detectability index is constant and the parameters c_b and p_0 in (A24)–(A25) can be adjusted to obtain an MMSE fit of $[A(N)/\sigma]_{\mathrm{bin}}$ to $[A(N)/\sigma]_{\mathrm{expt}}$. The resulting values of $[A(N)/\sigma]_{\mathrm{bin}}$ yield a much better fit to the dolphin data than can be obtained via linear summation or energy detection models.

The binary M-out-of-N receiver can be easily compared with linear summation for small SNR, which corresponds to a large number N of available echoes. For zero binary quantization threshold ($\gamma_b=0$) and for small SNR

$$p_0=1/2, \tag{A26}$$

and

$$\begin{aligned}p_1&=\mathrm{erfc}_*[(\gamma_b-A)/\sigma]\\&=\int_{-A/\sigma}^{\infty}(2\pi)^{-1/2}\exp(-y^2/2)dy\\&=(1/2)+\int_0^{A/\sigma}(2\pi)^{-1/2}\exp(-y^2/2)dy\\&\approx p_0+(A/\sigma)\left[(d/dx)\int_0^x(2\pi)^{-1/2}\exp(-y^2/2)dy\right]_{x=0}\\&=p_0+[A/(\sqrt{2\pi}\sigma)].\end{aligned} \tag{A27}$$

Substituting (A26) and (A27) into (A19) yields

$$d_b\approx\frac{\sqrt{N}A/\sigma}{\sqrt{\pi[(1/2)-(A/\sqrt{2\pi}\sigma)^2]}}\approx(2/\pi)^{1/2}d_l. \tag{A28}$$

At low SNR (large N), $d_b\approx 0.8d_l$. The performance of the binary M-out-of-N receiver is slightly worse than that of the linear summation receiver for a large number of echoes, and a slightly larger SNR should be required for detection. This comparison pertains to additive zero-mean Gaussian noise with known variance (known expected noise power). For non-Gaussian and/or nonstationary noise, the binary M-out-of-N receiver may be superior to linear summation.

For a small number of echoes, performance prediction of the binary M-out-of-N model involves a nonlinear transformation that greatly increases the required SNR. The binary summation data fit illustrated in Fig. 6 corresponds to $p_0=1/2$ and $c_b=0.999\,999\,3$ in (A25). The parameter c_b is written with high accuracy because a small change in c_b is associated with a large change in $\mathrm{erfc}_*^{-1}(p_1)$ when p_1 is close to unity. Substituting $p_0=1/2$, and $c_b=1.0$ into (A25), results in the equation

$$p_1=(1/2)+[2(1+N)]^{-1/2}. \tag{A29}$$

Substituting this expression for p_1 into (A24) with $p_0=1/2$ yields

$$[A(N)/\sigma]_{\mathrm{bin}}=-\mathrm{erfc}_*^{-1}\{(1/2)+[2(1+N)]^{-1/2}\}. \tag{A30}$$

The argument of the inverse complementary error function in (A30) is unity when N equals one and approaches $\frac{1}{2}$ as N becomes very large. As indicated in Fig. 5, the inverse complementary error function is unbounded when its argument equals zero, decreases monotonically as its argument increases, passes through zero when the argument is $\frac{1}{2}$, and goes to $-\infty$ when the argument equals 1,

$$\mathrm{erfc}_*^{-1}(0)=\infty;\quad \mathrm{erfc}_*^{-1}(1/2)=0;\quad \mathrm{erfc}_*^{-1}(1)=-\infty. \tag{A31}$$

Since c_b is slightly less than 1 for an MMSE fit to the data, the negative-inverse complementary error function is not unbounded for $N=1$, but is very large. This extremely nonlinear behavior allows the binary M-out-of-N model to closely approximate the large SNR required by the dolphin when only one echo is available ($N=1$).

Receiver comparisons can be further investigated by ROC (receiver operating characteristic) computation. The ROC is a plot of detection versus false-alarm probabilities for various threshold settings. For the binary M-out-of-N detector, threshold settings are limited to integer values of M between 1 and N. The probabilities of detection and false alarm for a given M value are

$$P_{D,M/N}=\sum_{k=M}^{N}\binom{N}{k}p_1^k(1-p_1)^{N-k},$$

$$p_1=\mathrm{erfc}_*[(\gamma_b-A)/\sigma], \tag{A32}$$

$$P_{F,M/N}=\sum_{k=M}^{N}\binom{N}{k}p_0^k(1-p_0)^{N-k},\quad p_0=\mathrm{erfc}_*(\gamma_b/\sigma). \tag{A33}$$

The false-alarm probability is independent of noise power σ^2 if the threshold for binary quantization γ_b equals zero. For zero γ_b, the false-alarm rate of the binary M-out-of-N receiver can be changed by adjusting the number of binary threshold crossings M that are required for detection. As M is increased, the false-alarm rate decreases, and the detection probability also decreases.

For linear summation

$$P_{D,\mathrm{lin}} = \mathrm{erfc}_*[\sqrt{N}(\gamma - A)/\sigma], \tag{A34}$$

$$P_{F,\mathrm{lin}} = \mathrm{erfc}_*(\sqrt{N}\gamma/\sigma). \tag{A35}$$

Dependence of the false-alarm rate on noise power can again be eliminated by setting the threshold of the linear receiver equal to zero. In the linear case, however, this threshold setting yields a large false-alarm rate that cannot be changed without introducing noise dependence. For linear summation with a constant false-alarm rate that is unequal to 0.5, noise power must be estimated and the threshold value must be adjusted accordingly.

Altes, R. A. (1995). "Signal processing for target recognition in biosonar," Neural Networks **8**, 1275–1295.

Altes, R. A. (2003). "Synthetic aperture and image sharpening models for animal sonar," *Echolocation in Bats and Dolphins*, edited by J. Thomas, C. Moss, and M. Vater (University of Chicago Press, Chicago), pp. 492–500.

Altes, R. A., Moore, P. W., and Helweg, D. A. (1998). "Tomographic image reconstruction of MCM targets using synthetic dolphin signals," Tech. Doc. 2993, Space and Naval Warfare Systems Center, San Diego, CA 921152-5001.

Au, W. W. L. (1993). *The Sonar of Dolphins* (Springer, New York).

Au, W. W. L., and Banks, K. (1998). "The acoustics of the snapping shrimp *Synalpheus parneomeris* in Kaneohe Bay," J. Acoust. Soc. Am. **103**, 41–47.

Au, W. W. L., and Moore, P. W. B. (1990). "Critical ratio and critical bandwidth for the Atlantic bottlenose dolphin," J. Acoust. Soc. Am. **88**, 1635–1638.

Au, W. W. L., Moore, P. W. B., and Pawloski, D. A. (1988). "Detection of complex echoes in noise by an echolocating dolphin," J. Acoust. Soc. Am. **83**(2), 662–668.

Brill, R. L., Moore, P. W. B., and Dankiewicz, L. A. (2001). "Assessment of dolphin (*Tursiops truncatus*) auditory sensitivity and hearing loss using jawphones," J. Acoust. Soc. Am. **109**(4), 1717–1722.

Bullock, T. H. (1986). "Significance of findings on electroreception for general neurobiology," in *Electroreception*, edited by T. H. Bullock and W. Heiligenberg (Wiley, New York), pp. 661–674.

Busnel, R.-G., and Fish, J. F., editors (1980). *Animal Sonar Systems* (Plenum, New York).

Colburn, H. S. (1996). "Computational models of binaural processing," in *Auditory Computation*, edited by H. L. Hawkins, T. A. McMullen, A. N. Popper, and R. R. Fay (Springer, New York), pp. 332–400.

Collett, D. (1952). *Modeling Binary Data*, 2nd ed. (Chapman and Hall/CRC, Boca Raton, 2003), pp. 56–57.

Dankiewicz, L. A., Helweg, D. A., Moore, P. W., and Zafran, J. M. (2002). "Discrimination of amplitude-modulated synthetic echo trains by an echolocating bottlenose dolphin," J. Acoust. Soc. Am. **112**, 1702–1708.

Ferguson, B. G., and Cleary, J. L. (2001). "*In situ* source level and source position estimates of biological transient signals produced by snapping shrimp in an underwater environment," J. Acoust. Soc. Am. **109**, 3031–3027.

Floyd, R. W. (1980). "Models of cetacean signal processing," in *Animal Sonar Systems*, edited by R. G. Busnel and J. F. Fish (Plenum, New York), pp. 615–623.

Gellermann, L. W. (1933). "Chance orders of alternating stimuli in visual discrimination experiments," J. Gen. Psychol. **42**, 206–208.

Green, D. M., and Swets, J. A. (1988). *Signal Detection Theory and Psychophysics* (Peninsula, Los Altos, CA).

Hagen, J. B., and Farley, D. T. (1973). "Digital-correlation techniques in radio science," Radio Sci. **8**, 775–784.

Hays, W. L. (1994). *Statistics*, 5th ed. (Harcourt-Brace, Fort Worth), pp. 597–660.

Helweg, D. A., Roitblat, H. L., Nachtigall, P. E., and Hautus, M. J. (1996). "Recognition of three-dimensional aspect-dependent objects by an echolocating bottlenosed dolphin," J. Exp. Psychol. Anim. Behav. Process **22**, 19–31.

Jeffress, L. A. (1948). "A place theory of sound localization," J. Comp. Physiol. Psychol. **41**, 35–39.

Johnson, C. S. (1968). "Masked tonal thresholds in the bottlenosed porpoise," J. Acoust. Soc. Am. **44**, 965–967.

Kedem, B. (1994). *Time Series Analysis by Higher Order Crossings* (IEEE, New York).

Konishi, M. (1993). "Listening with two ears," Sci. Am. **268**(4), 66–73.

Marr, D. (1982). *Vision* (Freeman, San Francisco).

Moore, P. W. B., Roitblat, H. L., Penner, R. H., and Nachtigall, P. E. (1991). "Recognizing successive dolphin echoes with an Integrator Gateway Network," Neural Networks **4**, 701–709.

Moore, P. W. B., and Schusterman, R. J. (1987). "Audiometric assessment of Northern fur seals, *Callorhinus ursinus*," Marine Mammal Sci. **3**, 31–53.

Mountain, D. C., and Hubbard, A. E. (1996). "Computational analysis of hair cell and auditory nerve processes," in *Auditory Computation*, edited by H. L. Hawkins, T. A. McMullen, A. N. Popper, and R. R. Fay (Springer, New York), pp. 121–156.

Nachtigall, P. E., and Moore, P. W. B., editors (1988). *Animal Sonar: Processes and Performance* (Plenum, New York).

Papoulis, A. (1965). *Probability, Random Variables, and Stochastic Processes* (McGraw-Hill, New York), pp. 102, 158.

Penner, R. H. (1988). "Attention and detection in dolphin echolocation," in *Animal Sonar: Processes and Performance*, edited by P. E. Nachtigall and P. W. B. Moore (Plenum, New York), pp. 707–713.

Requicha, A. (1980). "Zeros of entire functions," Proc. IEEE **68**, 308–328.

Roitblat, H. L., Moore, P. W. B., Nachtigall, P. E., and Penner, R. H. (1991). "Natural dolphin echo recognition using an Integrator Gateway Network," Adv. Neural Inf. Process. Systems **3**, 273–281.

Russell, I. J., Cody, A. R., and Richardson, G. P. (1986). "The responses of inner and outer hair cells in the turn of the guinea-pig cochlea and in the mouse cochlea grown *in vitro*," Hear. Res. **22**, 199–216.

Schafer, T. H., and Shewmaker, C. A. A. (1953). "A comparative study of the audio, visual and audio–visual recognition differentials for pulses masked by random noise," Naval Electronics Laboratory, Report 372.

Surlykke, A. (2003). "Detection thresholds depend on the number of echoes in the Big Brown Bat," *Echolocation in Bats and Dolphins*, edited by J. Thomas, C. Moss, and M. Vater (University of Chicago Press, Chicago), pp. 368–273.

Swets, J. A., and Green, D. M. (1964). "Sequential observations by human observers of signals in noise," in *Signal Detection and Recognition by Human Observers*, edited by J. A. Swets (Wiley, New York), pp. 221–242.

Swets, J. A., Shipley, E. F., McKey, M. J., and Green, D. M. (1964). "Multiple observations of signals in noise," in *Signal Detection and Recognition by Human Observers*, edited by J. A. Swets (Wiley, New York), pp. 201–220.

Thomas, J. A., and Kastelein, R. A., editors (1990). *Sensory Abilities of Cetaceans: Laboratory and Field Evidence* (Plenum, New York).

Urick, R. J. (1975). *Principles of Underwater Sound*, 2nd ed. (McGraw-Hill, New York), pp. 189–193.

Van Trees, H. L. (1968). *Detection, Estimation, and Modulation Theory* (Wiley, New York), pp. 36–38.

Vel'min, V. A., and Dubrovskiy, N. A. (1976). "The critical interval of active hearing in dolphins," Sov. Phys. Acoust. **22**, 351–352.

Versluis, M., Schmitz, B., von der Heydt, A., and Lohse, D. (2000). "How snapping shrimp snap: Through cavitating bubbles," Science **289**, 2114–2117.

Vetterli, M., and Kovacevic, J. (1995). *Wavelets and Subband Coding* (Prentice-Hall, Englewood Cliffs), pp. 208–213.

Viemeister, N. F., and Wakefield, G. H. (1991). "Temporal integration and multiple looks," J. Acoust. Soc. Am. **90**, 858–865.

Voelcker, H. (1966a). "Toward a unified theory of modulation, I," Proc. IEEE **54**, 340–353.

Voelcker, H. (1966b). "Toward a unified theory of modulation. II," Proc. IEEE **54**, 735–755.

Wolff, S. S., Thomas, J. B., and Williams, T. (1962). "The polarity coincidence correlator: A nonparametric detection device," IRE Trans. Inf. Theory **IT-8**, 1–19.